Structures and phase transition of multi-layered water nanotube confined to nanochannels†

Makoto Tadokoro,*[ab] Syoko Fukui,[b] Tadanori Kitajima,[b] Yuki Nagao,[c] Shin'ichi Ishimaru,[d] Hiroshi Kitagawa,[c] Kiyoshi Isobe[e] and Kazuhiro Nakasuji[f]

Received (in Cambridge, UK) 28th November 2005, Accepted 5th January 2006
First published as an Advance Article on the web 1st February 2006
DOI: 10.1039/b516807d

We placed nanometer-scale water-tube clusters with phase transition within a porous crystal formed from molecular blocks specifically designed to investigate the molecular dynamics of confined water molecules.

The dynamics and structure of water clusters[1] confined to a nanometer-scale environment are different from those of bulk water and ice under ambient pressure.[2] For example, intriguing theoretical studies have been carried out for a one-dimensionally ordered chain of water molecules,[3] and it was found that new ice phases not observed in bulk ice[4] are present within a carbon nanotube. Experiments have shown that a water decamer, representing a fragment model of the ice phase I_c, can be stabilized by noncovalent interactions.[5] The lowering of the freezing point of water confined to micropores such as those of zeolite,[6] and unusual viscosity on a thin water membrane bound to hydrophilic slits[7] were shown. Furthermore, neutron diffraction of a two-dimensional water cluster bound to molecular sheets[8] revealed an interesting behaviour at variable temperatures in relation to mutual interactions with the surface of the outer walls. We modelled the creation of a new nanometer-scale water cluster in a molecule-based nanoporous crystal in order to inspect the dynamics and behaviour of water molecules under specific conditions.

We recently employed crystal engineering, which is known as a method for controlling a crystal structure, to synthesize new molecular building blocks of H-bonded metal complexes having 2,2′-biimidazolate monoanion ($Hbim^{-1}$) as a ligand (Fig. 1S†).[9] This $Hbim^{-1}$ system controls the multi-dimensionality of molecular aggregations in the crystal by using difunctional ligands that are bonded to a metal by coordinate-covalent interactions and to each other by H-bonding interactions, as shown in Fig. 1a.[10] To confine water molecules within a nanometer-wide channel, we propose a new design strategy that introduces H-bonding donor or acceptor sites onto the surface of the channel framework. Thus, we used two types of building blocks, trimesic acid (TMA^{3-}) and $[Co^{III}(H_2bim)_3]^{3+}$, to construct a framework with mixed complementary intermolecular H-bonding between the building blocks. By comparing the relative acid–base strength of the corresponding chemical species, we predict that the complementary H-bonding is a proton-transferred H-bond (Fig. 1b) and not a neutral one (Fig. 1c).[11] The oxygen atoms of TMA^{3-} function as H-bonding acceptor sites for the water molecules. Furthermore, the strength of the mixed complementary H-bonding and the proton-accepting ability of the oxygen atoms may be enhanced in the ionic structure (Fig. 1b). This proton-transferred H-bonding structure is a new supramolecular synthon of H-bonding.[12]

The preparation was obtained by mixing H_3TMA and $[Co^{III}(H_2bim)_3](NO_3)_3$ in alkaline water. It was allowed to stand overnight at 45 °C, and we obtained orange crystals of **1** containing water molecules as a hexagonal prism with a framework of TMA^{3-} and $[Co^{III}(H_2bim)_3]^{3+}$ in a 1 : 1 ratio. In a similar manner, crystals of **2** containing D_2O were also prepared. Compound **2** is merely a deuterated version of **1**. Isolated crystals of **1** and **2** were susceptible to the escape of confined water (or heavy water) from the channels. Therefore, elemental analyses were performed on the crystals after dehydrating them by vacuum drying at 100 °C. The ratio of TMA^{3-} to $[Co^{III}(H_2bim)_3]^{3+}$ is 1 : 1.

We performed an X-ray crystal structure analysis of **1** at room temperature (23 °C) by placing **1** inside a glass capillary filled with water vapour.[13] The proton-transferred mixed complementary H-bonding generated two types of honeycomb sheets; Δ and Λ sheets between the Δ or Λ isomer of $[Co^{III}(H_2bim)_3]^{3+}$ and

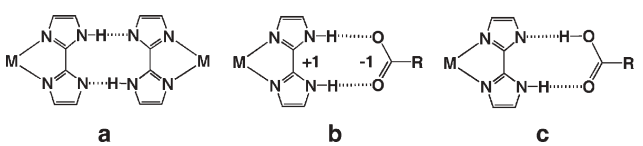

Fig. 1 (a) Complementary H-bonds with two sets of NH donors and N acceptors between neutral metal complexes with $Hbim^{-1}$ ligands, (b) ionic H-bonds between the anionic acid and the cationic H_2bim metal complex, and (c) the complementary neutral H-bonds between a carboxyl acid and a metal complex with $Hbim^{-1}$ ligands.

[a]*Department of Chemistry, Faculty of Science, Tokyo University of Science, Kagurazaka 1-3, Shinjuku-ku, Tokyo, Japan. E-mail: tadokoro@rs.kagu.tus.ac.jp; Fax: +81 3 3620 3858; Tel: +81 3 5228 8714*
[b]*Department of Chemistry, Graduate School of Science, Osaka City University, Sugimoto 3-3-138, Sumiyoshi-ku, Osaka, Japan. Fax: +81 6 6605 2522; Tel: +81 6 6605 2547*
[c]*Department of Chemistry, Graduate School of Science, Kyushu University, Hakozaki 6-10-1, Higashi-ku, Fukuoka, Japan. E-mail: hiroshiscc@mbox.nc.kyushu-u.ac.jp; Fax: +81 92-642-2570; Tel: +81 92-642-2570*
[d]*Department of Environmental Materials Science, School of Engineering, Tokyo Denki University, Takenisigakuenndai 2-1200, Inzei, Chiba, Japan. E-mail: ishimaru@cck.dendai.ac.jp; Fax: +81 476 46 8038; Tel: +81 476 46 8077*
[e]*Department of Chemistry, Graduate School of Science, Kanazawa University, Kadoma-cho, Kanazawa, Ishikawa, Japan. E-mail: isobe@cacheibm.s.kanazzawa-u.ac.jp; Fax: +81 76 264 5742; Tel: +81 76 264 5697*
[f]*Department of Chemistry, Graduate School of Science, Osaka University, Machikaneyama-cho 1-1, Toyonaka, Osaka, Japan. E-mail: nakasuji@chem.sci.osaka-u.ac.jp; Fax: +81 6 6850 5392; Tel: +81 6 6850 5392*

† Electronic supplementary information (ESI) available: experimental details. See DOI: 10.1039/b516807d

TMA^{3-}, respectively (Fig. 2a and 2b, and Fig. 2S†). The Δ and Λ sheets are stacked alternately along the *c* axis to realize the desired channel frameworks with H-bonding acceptor sites. The channel diameter, obtained by subtracting the van der Waals radius of the framework, is estimated to be approximately between 15 and 16 Å. The ratio of the channel volume to the unit cell volume is approximately 63%. The electron densities on the oxygen atoms of the water molecules are observed only near the outer wall of the channel, but these values cannot be accurately ascertained at this temperature due to the diffusion of the water molecules. (Figs. 3S and 4S†).

The existence of confined H_2O or D_2O molecules was also confirmed by thermogravimetry (TG) measurements, which were carried out after coating the fragile crystals **1** and **2** with paraffin liquid in air (Fig. 5S†). Hence, the number of H_2O and D_2O molecules for $[Co^{III}(H_2bim)_3](TMA)$ and $[Co^{III}(D_2bim)_3](TMA)$ units in crystals **1** and **2**, respectively, is determined to be more than twenty. Further, differential scanning calorimetry (DSC) thermograms were performed between −10 °C and −60 °C at a scan rate of 10 °C per min (Fig. 6S†). We observed a reversible phase transition for **1** and **2** that showed exothermic peaks at −38.8 °C and −33.4 °C, respectively, during cooling, and endothermic peaks at −28.3 °C and −22.8 °C, respectively, during heating. The difference in the temperatures of these phase transitions for **1** and **2** is almost comparable to the isotope effect (*ca.* ∼5 °C under ambient pressure)[14] on the freezing and melting of H_2O and D_2O. This similarity suggests that the peaks of the phase transitions in DSC are related to the condensation and fusion of water molecules within the channels. The irreversible endothermic peaks of **1** and **2** were also observed at 101.7 °C and 105.0 °C, respectively. The values of the freezing enthalpies[15] of **1** (65.89 cal mol^{-1}) and **2** (58.22 cal mol^{-1}) were rather low as compared with those of bulk ice (1436.3 cal mol^{-1}),[14] indicating that only a limited number of water molecules in the channels participate in the water–ice transition. Therefore, the strong H-bonded water molecules in the primary water tube probably play a less important role in this transition; this is because in the primary domain, these molecules are strongly H-bonded with the oxygen atoms of TMA^{3-} on the surface of the channels.

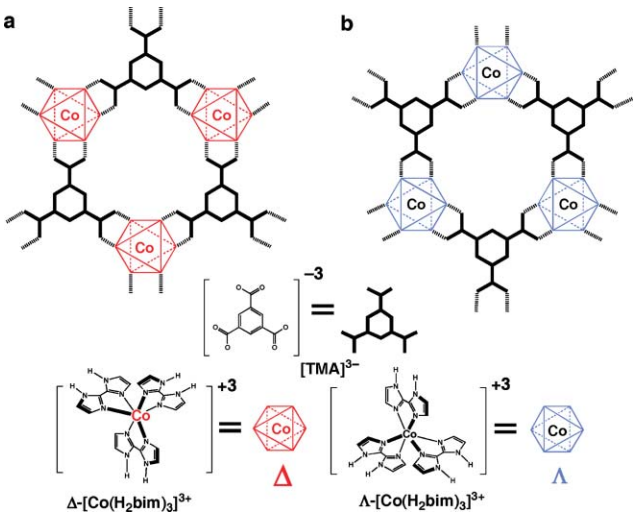

Fig. 2 Schematic representations of the H-bonding networks of Δ-sheet (a) and Λ-sheet (b).

We also performed X-ray crystal structure analysis below the phase transition temperature.[13] Figs. 3, 4 and 4S† show the crystal

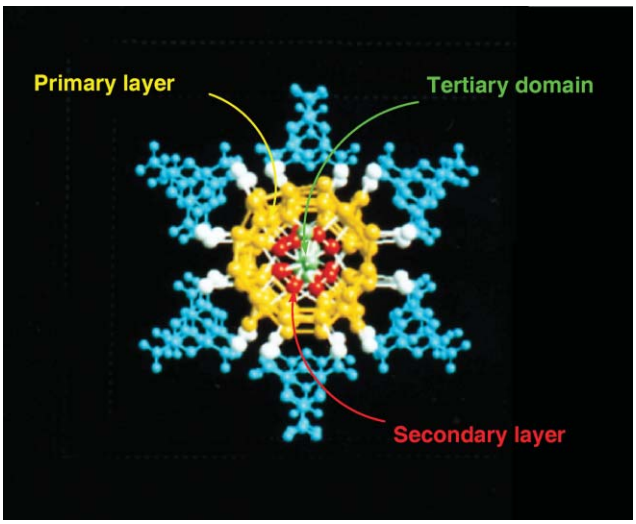

Fig. 3 A perspective view along the *c* axis of crystal structures for **1** below the phase transition temperature of −75 °C: the view of the multi-layered structure represents units of a channel-confining hierarchical ice-like tube. Trimesic acids contained in the outer wall of the channel as building blocks are shown by the blue spheres and solid lines. The yellow spheres and solid lines describe H-bonding between water molecules in the primary layer stabilized by strong interactions with the oxygen atoms (white spheres) of the trimesic acid of the outer wall. For clarity, H-bonding greater than 2.7 Å (*i.e.*, the mean value of H-bonding distance) was omitted. The red spheres and solid lines represent H-bonding between water molecules in the secondary layer, and the green spheres show water molecules in the tertiary domain, respectively.

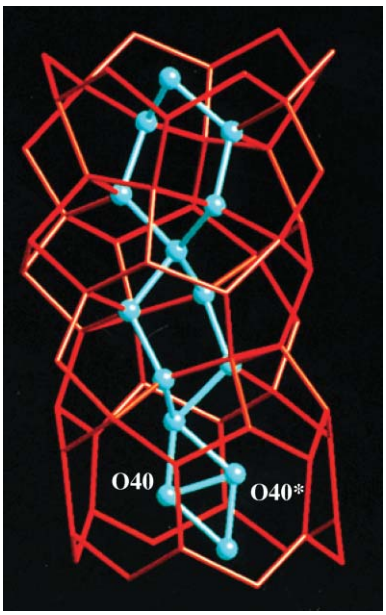

Fig. 4 A view of the crystal structure for a unit of the three-layered ice nanotube into **1** below the phase transition temperature of −75 °C. The red solid lines describe H-bonding between water molecules in the primary water-tube. The blue spheres and solid lines represent H-bonding between water molecules in the secondary water-layer and the tertiary water domain.

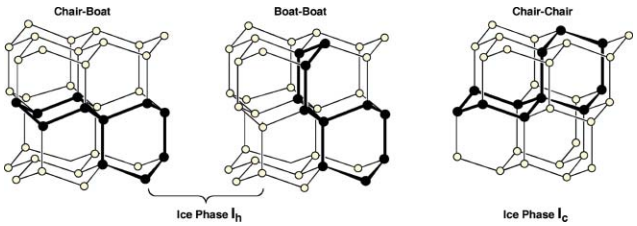

Fig. 5 The spiro-bihexagon units found in the hydrogen bonding structure of two ice polymorphs of ice phases I_h and I_c: I_h is constructed from two patterns of the chair-boat and boat-boat conformations, while, I_c is constructed from only one pattern of the chair–chair conformation.

structure of the hierarchical ice-like tube containing **1** at −75 °C. The confined water molecules are recognized as a certain type of "multi-layered ice" composed of three-layered nanotube networks. At −75 °C, the *c* axis of the crystal is three times as long as that at 23 °C; we believe that this is due to formation of the ice nanotube. Thus, the structure of the water nanotube at 23 °C would be essentially different from that of the ice nanotube. Such H-bonded ice nanotube networks are held in the channel by additional H-bonds between the water molecules in the primary water tube and the oxygen atoms of TMA^{3-} on the surface of the framework, primary water tube, secondary water layer, and tertiary water segment, as shown in Fig. 3S†. The H-bonded networks in the primary layer are constructed from small cyclic structures; such as pentagons, hexagons and octagons; they are also held to the oxygen atoms on the channel framework by H-bonds. The octagonal structure was not found in a normal clathrate hydrate.[16] Interestingly, the secondary and tertiary water domains consist of a poly-spiro chain in which a disordered water molecule and two spiro hexagons are connected to each other by H-bonds (Fig. 4). All the hexagons of the spiro chain have a chair–chair conformation; this is found only in the fragment of the cubic ice phase I_c and not in a hexagonal phase I_h, which comprises spiro structures with chair–boat and boat–boat conformations (Fig. 5).[17] The ice phase I_c is known to be stable below −80 °C at atmospheric pressure.[18] The spiro-bihexagon unit found in this study is expected to be a suitable model for crystal embryo formation at the ice phase I_c during heterogeneous nucleation; further, it may also provide important information concerning ice growth in this I_c phase under extreme conditions. A water molecule that is still disordered at this temperature exists in the connection between the spiro-bihexagons in the nanotube (O(40) and O(40)*). In the two sites, one disordering water molecule is located in the water cluster of a cyclic belt-like hexagon that belongs to the primary layer. Since the cyclic belt-like cluster consists of an exclusive space surrounded by six condensed hexagons, the disordered water molecule would not condense for the normal ice formation even at −75 °C. Thus, a repeating unit of the ice nanotube is constructed for obtaining a large water cluster with 60 H_2O molecules that are connected by H-bonds. (The primary tube is formed from 48 H_2O molecules, and the secondary and tertiary portions are formed from a total of 12 H_2O molecules.) On the other hand, at a low temperature, *i.e.*, less than −75 °C, an X-ray analysis for **1** reveals that it is now very difficult to form a twin crystal as the temperature decreases. In future, it is necessary to reveal the crystal structure of the ice nanotube in the lower temperature region.

In this study, we have created a novel water-tube network anchored in a 1D nanometer-scale channel framework. The channels were constructed by designing molecular building blocks for a new supramolecular synthon. The water molecules within the tube structure demonstrate the intriguing tube-like ice-water phase transition. This transition is caused by water molecules in the secondary and tertiary domains, where dynamic structural changes occur. In addition, water molecules in the secondary and tertiary domains assist in generating the spiro-bihexagon and disordered water molecule, which are stabilized by H-bonding below the transition temperature. Above this temperature, the networks transform to a highly disordered species, as observed by the X-ray analysis. These findings represent the first reported description of this unexpected property of water. Studies on confined water are relevant to a number of biological processes including hydration of a biological surface,[18] dynamics of hydrated proteins,[19] and the mobility of water within biological pores.[20] Thus, our synthetic efforts using crystal engineering may contribute to a greater understanding of the ice formation mechanism and the properties of water and ice in a biological context.

Notes and references

1 F. N. Keutsch and R. J. Saykally, *Proc. Natl. Acad. Sci. U. S. A.*, 2001, **98**, 10533; K. Liu, J. D. Cruzan and R. J. Saykally, *Science*, 1996, **271**, 929; R. Ludwig, *Angew. Chem., Int. Ed.*, 2001, **40**, 1808.
2 T. Ohba, K. Kanoh and K. Kaneko, *J. Am. Chem. Soc.*, 2004, **126**, 1560; J. H. Walther, R. Jaffe, T. Halicioglu and P. Koumoutsakos, *J. Phys. Chem. B*, 2001, **105**, 9980.
3 K. Koga, G. T. Gao, H. Tanaka and X. C. Zeng, *Nature*, 2001, **412**, 802.
4 G. Hummer, J. C. Rasaiah and J. P. Noworyta, *Nature*, 2001, **412**, 188.
5 L. J. Barbour, G. W. Orr and J. L. Atwood, *Nature*, 1998, **393**, 671; L. J. Barbour, G. W. Orr and J. L. Atwood, *Chem. Commun.*, 2000, 859.
6 U. Raviv, P. Laurat and J. Klein, *Nature*, 2001, **413**, 51.
7 R. G. Horn, D. T. Smith and W. Haller, *Chem. Phys. Lett.*, 1989, **162**, 404.
8 C. Janiak, T. G. Scharmann and S. A. Mason, *J. Am. Chem. Soc.*, 2002, **124**, 14010.
9 M. Tadokoro, H. Kanno, T. Kitajima, H. S. Umemoto, N. Nakanishi, K. Isobe and K. Nakasuji, *Proc. Natl. Acad. Sci. U. S. A.*, 2002, **99**, 4950.
10 R. Atencio, M. Chacón, T. González, A. Briceno, G. Agrifoglio and A. Sierralta, *Dalton Trans.*, 2004, 505.
11 M. Tadokoro and K. Nakasuji, *Coord. Chem. Rev.*, 2000, **198**, 205.
12 G. R. Desiraju, *Angew. Chem., Int. Ed. Engl.*, 1995, **34**, 2311.
13 Single crystal **1** of this material at 23.0 °C are $C_{27}H_{67}N_{12}O_{29}Co$, *Fw* = 1082.28, monoclinic of space group *C*2/*c* (no. 15), with cell dimensions; *a* = 16.403(5) Å, *b* = 29.471(7) Å, *c* = 10.954 (6) Å, *β* = 90.24(3)°; *V* = 5295(3) Å^3 and *Z* = 4, D_{calcd} = 1.358 g cm^{-3}, μ(Mo-Kα) = 4.18 cm^{-1}, *R* = 8.80%, GOF = 1.23. (*R* = 5.43%, treated in the Platon SQUEEZE routine to remove the water molecules). Single crystal data of **1** at −75.0 °C are $C_{81}H_{183}N_{36}O_{78}Co_3$, *Fw* = 3086.42, monoclinic of space group *C*2/*c* (no. 15), with cell dimensions; *a* = 16.726(2) Å, *b* = 29.142(3) Å, *c* = 32.264 (3) Å, *β* = 92.939(4)°; *V* = 15705(3) Å^3 and *Z* = 4, D_{calcd} = 1.305 g cm^{-3}, μ(Mo-Kα) = 4.16 cm^{-1}, *R* = 9.50%, GOF = 1.09. The crystal structures of the two principal components at 23 °C lie about two-fold axes. The crystal structure of Co(1) at −75 °C is in a general position, and that of Co(2) and one of the trimesic acid molecules lie on two-fold axes. CCDC-286770 and 292075 at 23 °C and 220823 at −75 °C. For crystallographic data in CIF or other electronic format see DOI: 10.1039/b516807d.
14 D. Eisenberg and W. J. Kauzmann, *The structure and properties of water*, Oxford at the Clarendon Press, London, 1969.
15 These values were calculated using the number of water molecules determined by X-ray analysis of **1** below the transition temperature.
16 E. D. Sloan, Jr., *Nature*, 2003, **426**, 353.
17 M. Matsumoto, S. Saito and I. Ohmine, *Nature*, 2002, **416**, 409.
18 M. S. P. Sansom and P. C. Biggin, *Nature*, 2001, **414**, 156.
19 M. Settles and W. Doster, *Faraday Discuss.*, 1996, **103**, 269.
20 Y. Zhou, J. H. Morais-Cabral, A. Kaufman and R. MacKinnon, *Nature*, 2001, **414**, 43.